



Molecular Characterization and RNA Interference Analysis of SLC26A10 From *Nilaparvata lugens* (Stål)

Ruijuan Zhang, Jinliang Ji, Yabin Li, Jianbin Yu, Xiaoping Yu and Yipeng Xu*

Zhejiang Provincial Key Laboratory of Biometrology and Inspection and Quarantine, College of Life Sciences, China Jiliang University, Hangzhou, China

SLC26A10 is a member of the SLC26 gene family, but its role in insects is still unclear. We cloned the *SLC26A10* gene of *Nilaparvata lugens* (*NISLC26A10*) and found *NISLC26A10* contained 11 transmembrane regions and a STAS domain. Expression pattern analysis showed *NISLC26A10* expression was more upregulated in adults than in nymphs, highest in the ovary. After injection of double-stranded RNA (dsRNA) of *NISLC26A10*, the mRNA level of *NISLC26A10* significantly decreased and, consequently, the ovarian development of adult females was hindered; the amount and the hatchability of eggs and yeast-like symbionts in mature oocytes decreased. Further study showed that *NISLC26A10* might result in decreased juvenile hormone level and vitellogenin expression. These results indicate that *NISLC26A10* plays an essential role in the reproduction of *N. lugens*.

Keywords: *Nilaparvata lugens*, SLC26A10, RNAi, ovarian development, reproduction

OPEN ACCESS

Edited by:

Amit Roy,
Czech University of Life Sciences
Prague, Czechia

Reviewed by:

Huizhen Guo,
Southwest University, China
Smitha George,
Dalhousie University, Canada

*Correspondence:

Yipeng Xu
xyp@cjlu.edu.cn

Specialty section:

This article was submitted to
Invertebrate Physiology,
a section of the journal
Frontiers in Physiology

Received: 13 January 2022

Accepted: 17 February 2022

Published: 17 March 2022

Citation:

Zhang R, Ji J, Li Y, Yu J, Yu X and
Xu Y (2022) Molecular
Characterization and RNA
Interference Analysis of SLC26A10
From *Nilaparvata lugens* (Stål).
Front. Physiol. 13:853956.
doi: 10.3389/fphys.2022.853956

INTRODUCTION

The brown planthopper, *Nilaparvata lugens* Stål (Hemiptera: Delphacidae), is a devastating insect pest of rice in Asia (Heong and Hardy, 2009). *N. lugens* sucks phloem sap and spreads viruses, seriously harming the plant (Sōgawa, 1982; Zheng et al., 2014). In recent years, outbreaks of *N. lugens* have been continuously recorded, causing 1–1.5 billion kilograms of rice production losses per year in China. As an *r*-reproductive strategy insect, *N. lugens* has a strong adaptability to develop resistance to chemical insecticides or resistant rice varieties, making it hard to be controlled. Therefore, it is urgently needed to study new control strategies of *N. lugens* (Bottrell and Schoenly, 2012). A control strategy is to identify genes that play vital roles in the growth and development of *N. lugens* and use these genes as targets. For example, RNA interference (RNAi) is an effective alternative technique for controlling *N. lugens* based on target genes (Whitfield and Rotenberg, 2015; Bao and Zhang, 2019).

Solute carrier family 26 (SLC26) is a conserved multifunctional anion exchanger family with 11 members (SLC26A1–SLC26A11), involved in anions secretion and absorption. The SLC26 family members contain transmembrane regions and a C-terminal STAS domain (sulfate transporter and anti-sigma factor antagonist; Wang et al., 2019). Most members of the SLC26 family act as anion exchangers, only SLC26A7 and SLC26A9 have been shown to act as anion channels alone. Because the SLC26 family was newly found in recent years,

the functions of its members have not been well explored, and only some general features and potential cellular function have been introduced. Members of the SLC26 family have been reported to be associated with several diseases and symptoms, including multiple epiphyseal dysplasia (SLC26A2), congenital chloride diarrhea (Slc26A3), Pendred syndrome (SLC26A4), nonsyndromic (isolated) hearing impairment (SLC26A5), calcium oxalate kidney stones (SLC26A6), congenital hypothyroidism (SLC26A7), male infertility (SLC26A8), and gastric hypochlorhydria (SLC26A9; Sindić et al., 2007; Ohana et al., 2009; Alper and Sharma, 2013). Until to now, the physiological roles of SLC26A1, SLC26A10, and SLC26A11 have not been reported. As a member of the SLC26 family, SLC26A10 (SLC26 member 10) has been reported in mammals, including humans (Mount and Romero, 2004), mice (Alvarez et al., 2004), guinea pigs (Andharia et al., 2018), and Australian sheep (Knight et al., 2012), but its function is still unclear.

In our previous experiment, we found *SLC26A10* was highly expressed in ovaries during a transcriptome analysis of *N. lugens*. This implied that *SLC26A10* might play an important role in the ovarian development of *N. lugens*. In the present study, we cloned *SLC26A10* of *N. lugens*, performed bioinformatics analysis, and examined the expression patterns of *NISLC26A10* by qPCR. Furthermore, we studied the function of *SLC26A10* in *N. lugens* by RNAi.

MATERIALS AND METHODS

Tested Insects

Nilaparvata lugens used for this study were maintained in a climatron at China Jiliang University, Hangzhou, China. The population of *N. lugens* was reared on rice TN1, at 27±1°C, with a 16:8h (light:dark) photoperiod.

Extraction of Total RNA and Cloning of *NISLC26A10*

Total RNA was extracted from *N. lugens* adult females with TRIzol Reagent (Takara, Dalian, China), following the manufacturer's instructions. After verifying the integrity and measuring the concentration of RNA, 1 µg total RNA was used for cDNA synthesis with a PrimeScript™ II first Strand cDNA Synthesis Kit (Takara, Dalian, China). A pair of primers (*NISLC26A10*-F and *NISLC26A10*-R; **Supplementary Table S1**) was designed with Primer Premier 5.0 software and we amplified the *NISLC26A10* sequence using Premix Taq™ (LA Taq™ Version 2.0, Takara, Dalian, China). Then, the PCR product was cloned into the pMD™19-T vector (Takara, Dalian, China) and sequenced.

Sequence Analysis

The open reading frame (ORF) of *NISLC26A10* was predicted using the ORF Finder. Its isoelectric point (*pI*) and molecular weight (*Mw*) were predicted with ExpASY.¹ The signal peptide

and transmembrane helices were predicted with SignalP² and TMHMM Server v. 2.0,³ respectively. The protein domain was predicted with HMMER.⁴ The *NISLC26A10* protein sequence was compared with other SLC26A10 sequences in the NCBI database.⁵ Multiple sequences were aligned by DNAMAN software. The evolutionary tree was constructed with the neighbor-joining method using MEGA 10.2.

Real-Time Quantitative PCR Analysis

The mRNA level of *NISLC26A10* was analyzed by real-time quantitative PCR (qPCR). Total RNA of samples was extracted, and 1 µg total RNA was used for cDNA synthesis with a Perfect Real-Time PrimeScript™ RT reagent Kit with gDNA Eraser (Takara, Dalian, China). Pairs of primers for qPCR analysis of target genes were designed with Primer Premier 5.0 software (**Supplementary Table S1**), and their specificity was confirmed by the agarose gel electrophoresis and melt curve analysis of the qPCR product. The qPCR was performed in 20 µl reactions, including 10 µl TB Green® Premix Ex Taq™ II (Tli RNaseH Plus; Takara, Dalian, China), 1 µl each primer (10 µM), 2 µl cDNA template, and 5.6 µl ultrapure water. The program of qPCR was 94°C for 30 s, and 40 cycles of 94°C for 5 s and 60°C for 30 s. The expression level of *NISLC26A10* was evaluated by the 2^{-ΔΔCt} method, taking the *N. lugens* 18S rRNA (*Nl18S*) as the internal control gene (Wu et al., 2019).

RNA Interference

A pair of primers (T7-*NISLC26A10*-dsF and T7-*NISLC26A10*-dsR) that contained a T7 polymerase promoter was designed for amplifying the DNA template of *SLC26A10* dsRNA (ds*SLC26A10*; **Supplementary Table S1**; Milligan et al., 1987; Wu et al., 2019). The DNA template was 591 bp; dsRNA of the GFP gene (ds*GFP*) was used as the negative control. The GFP gene sequence was synthesized *in vitro* and referred to as the binary vector pCAMBIA-1,302 (GenBank: AF234298.1). The primers for synthesizing ds*GFP* were T7-*GFP*-dsF and T7-*GFP*-dsR, and the DNA template for ds*GFP* synthesis was 350 bp. The dsRNA was synthesized by an Invitrogen™ MEGAscript™ T7 Transcription Kit (Ambion, Austin, TX, United States), following the manufacturer's instructions. The integrity of synthesized dsRNA was verified by 1% agarose gel electrophoresis and its concentration of RNA was measured by a NanoDrop 2000 system (Thermo Fisher Scientific, Waltham, MA, United States).

RNAi was performed by dsRNA injection. Newly emerged virgin female adults were anesthetized with ice for 40–50 s and about 50 nl of dsRNA (5,000 ng/µl) was injected into the abdomen using a manual microinjector.

²<http://www.cbs.dtu.dk/services/SignalP/>

³<http://www.cbs.dtu.dk/services/TMHMM>

⁴<https://www.ebi.ac.uk/Tools/hmmer/>

⁵<https://www.ncbi.nlm.nih.gov/>

¹http://web.expasy.org/compute_pi/

Dissection Observation and Fertility Analysis

The healthy individual females injected with dsRNA were transferred to fresh rice seedlings in a jar with two untreated male adults. To count the number of eggs, fresh rice seedlings were changed every day until the females died. The survival rate of female adults and the number of eggs (hatched and unhatched) were counted. For dissection, insects treated with dsRNA were anesthetized on ice and then, the cuticle was carefully removed. The tissues in PBS were imaged under a stereo zoom microscope (Nikon SMZ1500, Tokyo, Japan), photographed with NIS Elements software.

Quantity Statistics of Yeast-Like Symbionts in Mature Oocytes

Yeast-like symbionts (YLSs) are primary symbionts of *N. lugens* (Noda et al., 1995) and are transovarially transmitted in the *N. lugens* population (Houk and Griffiths, 1980). The YLSs enter the oocyte through ovarian epithelial plug and develop into bacteriocytes in the posterior end of the oocyte after oocyte maturation (Cheng and Hou, 2001). The number of YLSs in the mature oocyte of *N. lugens* was counted after dsRNA injection. After dissection from the female adults, the mature oocytes were treated with 35% sodium hypochlorite solution. Then, the bacteriocytes were released from the posterior end of the oocytes, and the YLSs were released from the bacteriocytes. After YLSs were well spread in the solution, they were imaged under a Nikon inverted microscope (ECLIPSE Ti-S, Tokyo, Japan), photographed with NIS Elements software.

Immunofluorescence Analysis

Immunofluorescence was used to analyze the localization and distribution of target proteins. The immunofluorescence staining was carried out as described previously (Nan et al., 2016). The primary antibody (Anti-SLC26A10) was a rabbit polyclonal antibody against a polypeptide (ENDPLLGNE DSGGK) of *NISLC26A10* deduced protein. The specificity of the primary antibody has been verified by Western blot. The secondary antibody was goat anti-rabbit IgG antibody conjugated with Dylight 488 fluorescent dye (Abbkine, California, USA). Samples were imaged and photographed with Laser Scanning Confocal Microscope (Leica SP8, Mannheim, Germany).

RESULTS

Identification and Phylogenetic Analysis of *NISLC26A10*

NISLC26A10 has an 1872bp ORF that encodes a protein of 623 amino acid residues (GenBank: OM282973) with a calculated molecular mass of 68.2kDa and an isoelectric point (*pI*) of 6.51, without signal peptides. As expected, *NISLC26A10* contains 11 transmembrane regions and a STAS domain (Figure 1). Sequence comparison and phylogenetic analysis show that SLC26A10s are conserved in animals (Supplementary Figure S1; Figure 2), indicating SLC26A10 has some basic functions in insects.

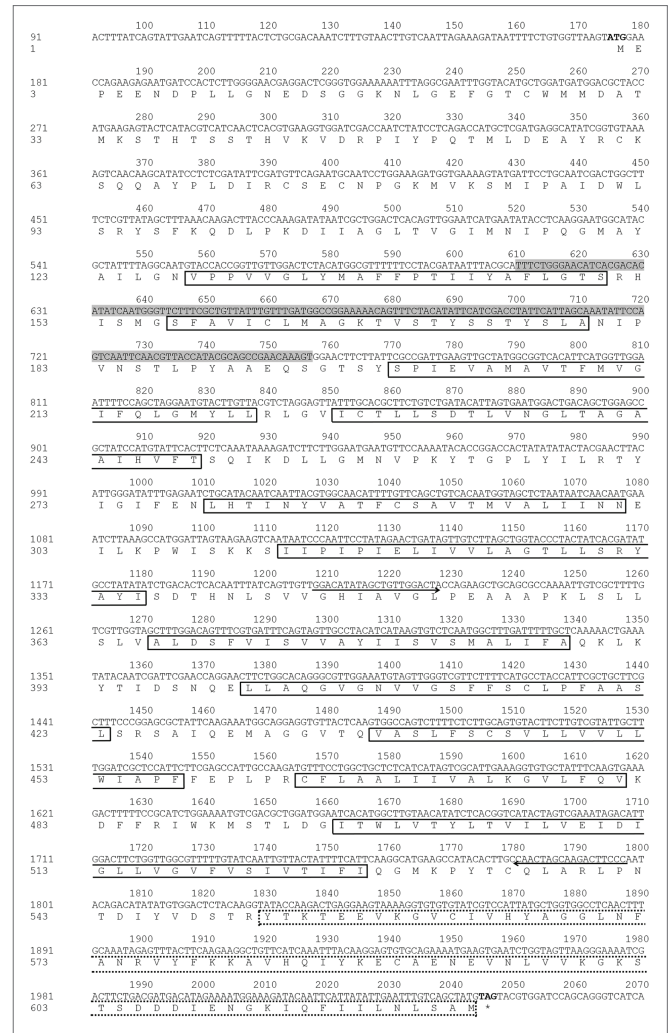


FIGURE 1 | Nucleotide and deduced amino acid sequence of *NISLC26A10*. The start codon (ATG) and stop codon (TAG) are in bold. The primers used for amplifying the DNA template of dsRNA are shown with direction arrows. The template sequence for qPCR is shown in the shadowed area. The 11 transmembrane regions are shown in full-lined boxes, and STAS (552–623 aa) is shown in a dot-lined box.

Temporospatial Expression Pattern of *NISLC26A10*

The expression pattern of *NISLC26A10* was analyzed by qPCR (Figure 3). *NISLC26A10* was expressed in all developmental stages, and its expression level in nymphs and female adults was higher (Figure 3A). *NISLC26A10* was expressed in all tested tissues, including the head, thorax, fat body, gut, and ovary. Among these tissues, *NISLC26A10* expression was highest in the ovary, followed by the gut (Figure 3B).

Effects of RNA Interference

To detect the interference efficiency of ds*NISLC26A10*, female adults at 2, 3, and 5 days post-injection of dsRNA (d.p.i.) were collected. qPCR results showed that *NISLC26A10*

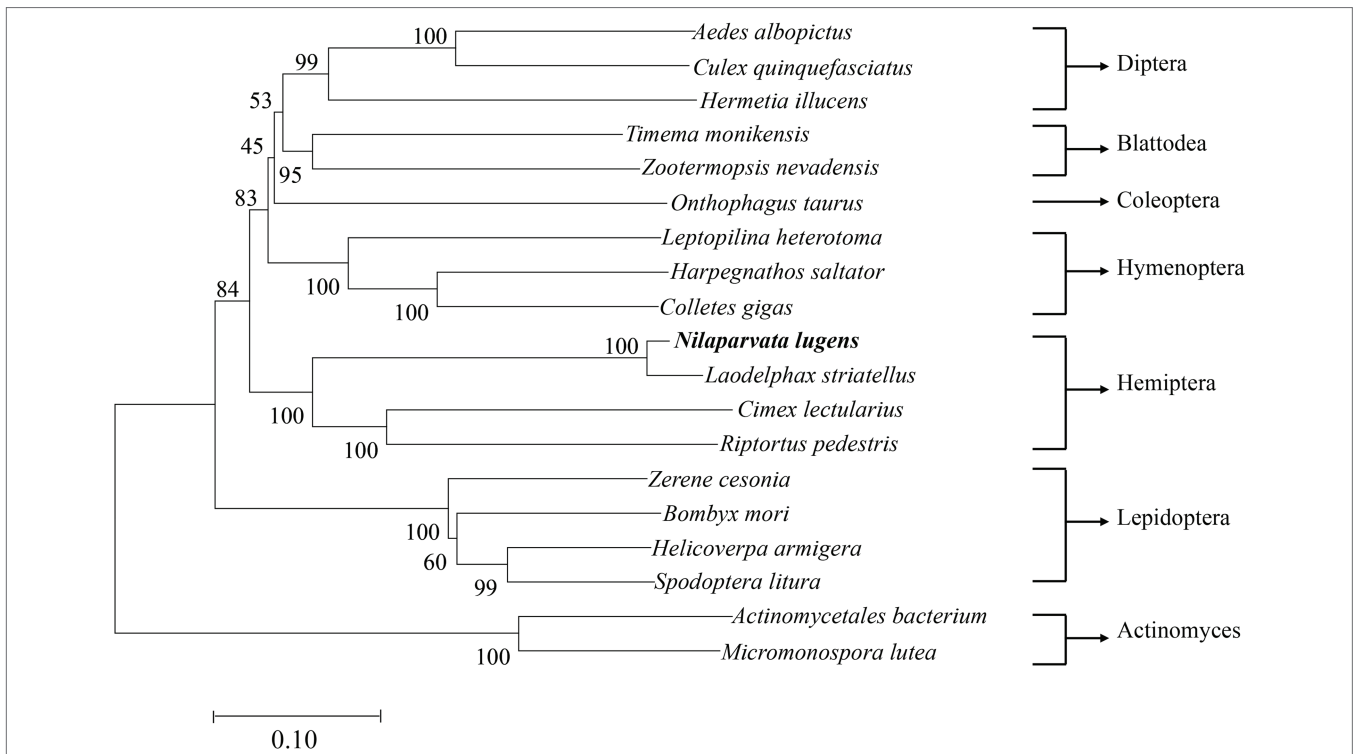


FIGURE 2 | The diagram of phylogenetic relationships of NISLC26A10. The analysis involved 19 nucleotide sequences, *Actinomycetales bacterium* and *Micromonospora lutea* were used as outgroups. The bootstrap of trees was 1,000 replicates. *Nilaparvata lugens* and *Laodelphax striatellus* are closely related. *Aedes albopictus*, XP 029731531.1; *Culex quinquefasciatus*, XP 038112203.1; *Hermetia illucens*, XP 037917492.1; *Timema monikensis*, CAD7432363.1; *Zootermopsis nevadensis*, XP 021939110.1; *Onthophagus taurus*, XP 022906818.1; *Leptopilina heterotoma*, XP 043475130.1; *Harpegnathos saltator*, XP 011151869.1; *Colletes gigas*, XP 043248168.1; *Laodelphax striatellus*, RZF38072.1; *Cimex lectularius*, XP 014247282.1; *Riptortus pedestris*, BAN20811.1; *Zerene cesonia*, XP 038213017.1; *Bombyx mori*, XP 021205545.1; *Helicoverpa armigera*, XP 021191371.1; *Spodoptera litura*, XP 022831360.1; *Actinomycetales bacterium*, NLT53914.1; and *Micromonospora lutea*, WP 204001039.1.

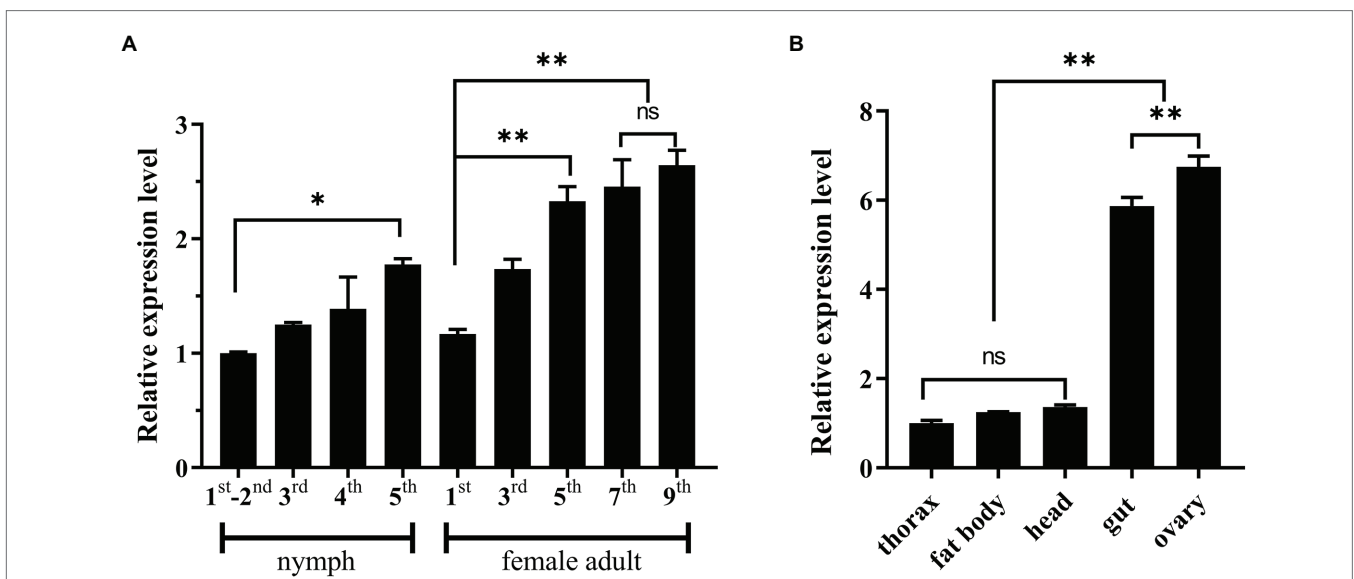
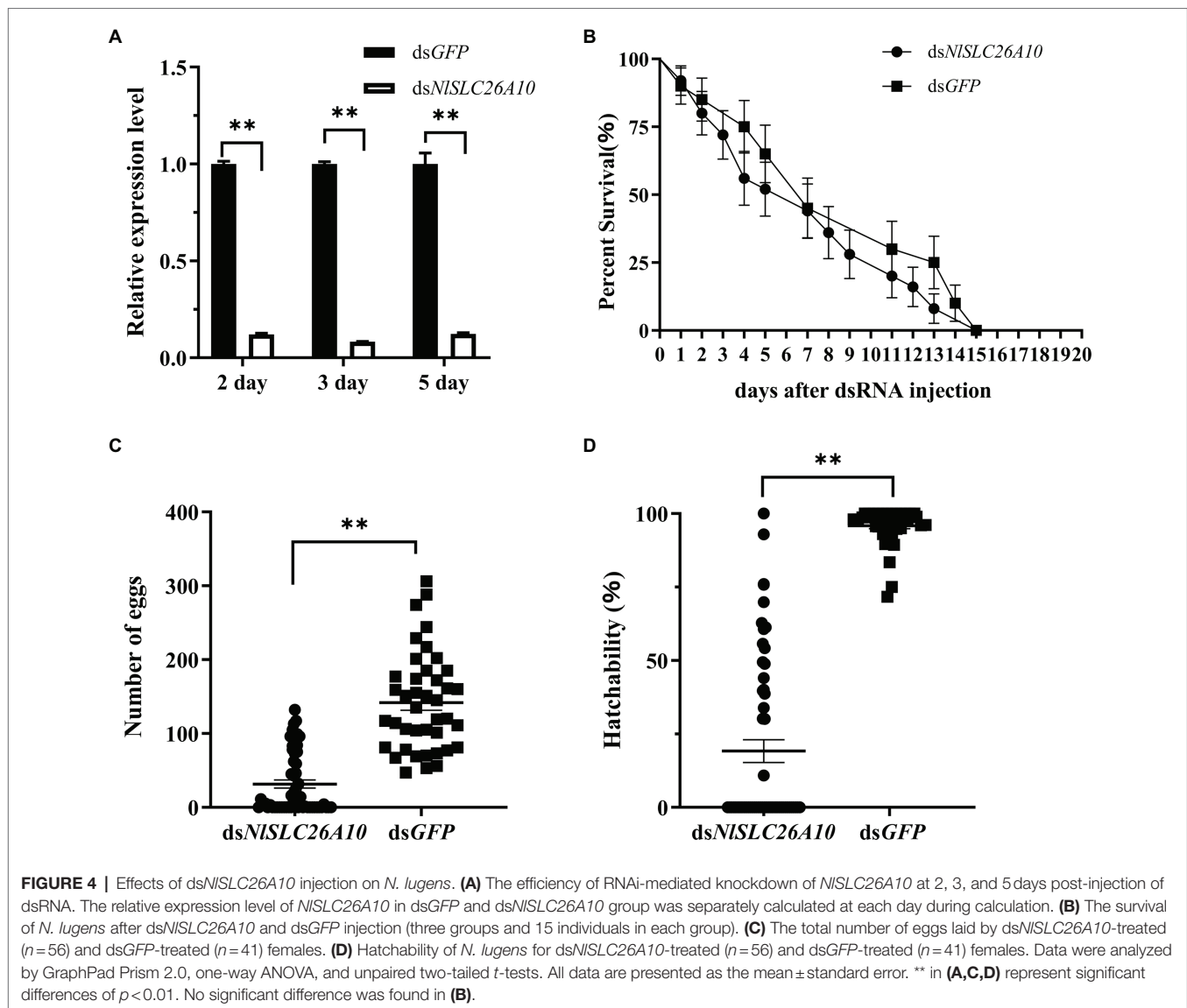


FIGURE 3 | Expression patterns of *NISLC26A10*. **(A)** Temporal expression pattern of *NISLC26A10*. Developmental stages include 1–5 instars of nymphs and 1–9 day old female adults. **(B)** Tissue expression patterns of *NISLC26A10* in five tissues of female adults. All data are presented as the mean ± standard error (Data were analyzed by GraphPad Prism 2.0 and one-way ANOVA). Significant difference: * means $p < 0.05$, ** means $p < 0.01$, and ns means no significance.



expression was significantly downregulated by 87.9, 91.7, and 87.8% at 2, 3, and 5 d.p.i., respectively, showing that RNAi-mediated knockdown of *NISLC26A10* was effective (Figure 4A).

Effects of RNAi on the Survival of *N. lugens*

The number of the living individuals until 20 d.p.i. was recorded. The results showed that there was no obvious difference in survival rate between dsNISLC26A10 and dsGFP treatments (Figure 4B), confirming dsNISLC26A10 had no lethal effect on *N. lugens*.

Effects of RNAi on the Laying of Eggs

The total number of eggs (hatched and unhatched) laid by dsNISLC26A10-treated and dsGFP-treated female adults within 20 days were counted. After dsGFP injection, three-quarters of female adults laid more than 100 eggs and the average number

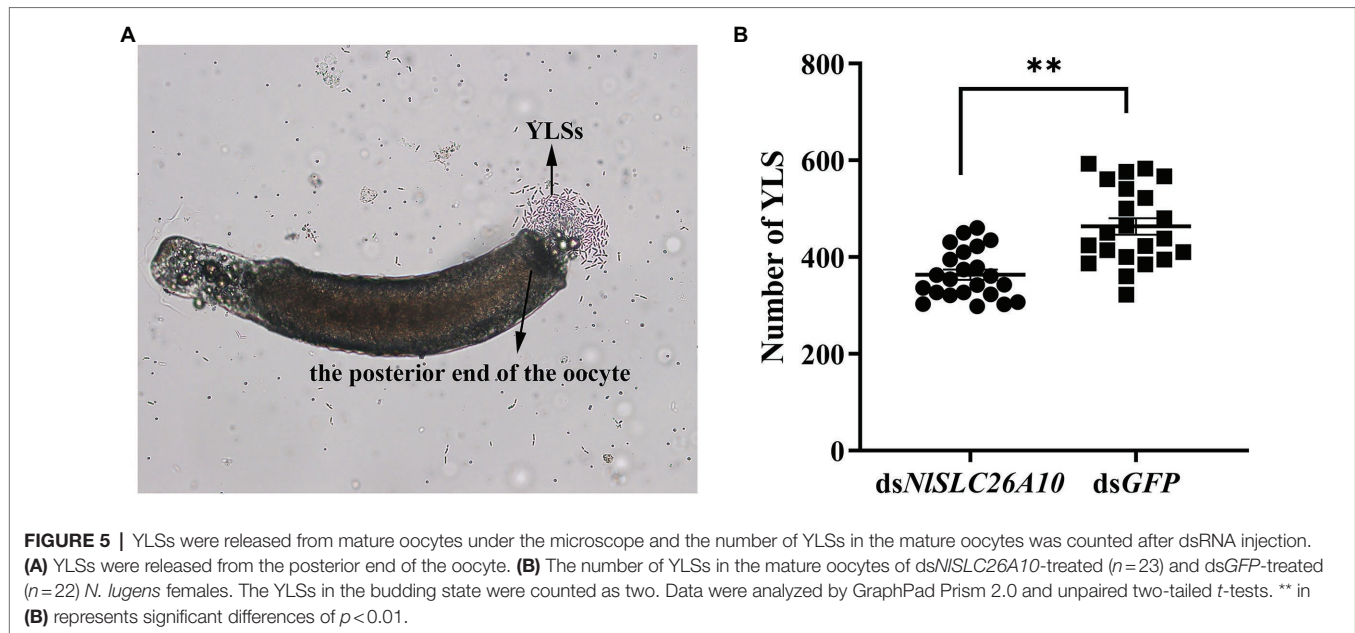
of eggs was 142. Injected with dsNISLC26A10, two-fifths of female adults laid no egg and the average number of eggs was 32 (Figure 4C). The hatchability of eggs laid by dsNISLC26A10-treated females was much less than that of dsGFP-treated (Figure 4D). These results indicate dsNISLC26A10 injection affects the spawning and egg hatching of *N. lugens*.

Effects of RNAi on the Number of YLSs

In addition, the number of YLSs in the mature oocytes of *N. lugens* at 5 d.p.i. was recorded. The results showed the number of YLSs from the dsNISLC26A10 treatment was lower than dsGFP (Figure 5), demonstrating that the injection of dsNISLC26A10 affects YLSs entering *N. lugens* oocytes.

Effects of RNAi on Ovary Development

The female adults at 1–5 d.p.i. were dissected. Within 1–3 d.p.i., there was no obvious difference in most ovaries between



ds*NISLC26A10*-treated and ds*GFP*-treated. However, the difference was obvious at 5 d.p.i. At this time, ovaries of ds*GFP*-treated were matured, fully developed, and banana-shaped (**Figure 6A**), but in ds*NISLC26A10*-treated females, most ovaries were small, poorly developed, had fewer mature oocytes, and remained immature up to 5 d.p.i. (**Figures 6B–D**). The results demonstrate that *NISLC26A10* is related to the ovarian development of *N. lugens*.

Immunofluorescence Analysis of *NISLC26A10* Expression

To detect the expression of *NISLC26A10* in *N. lugens*, immunofluorescence staining was performed. The expression of *NISLC26A10* was observed in the ovary (**Figures 7A,B**) and gut (**Figures 7C,D**). *NISLC26A10* was more highly expressed in the ovariole pedicel. As shown, *NISLC26A10* was localized on the cytomembrane (**Figures 8B,D'**), consistent with the bioinformatics analysis result that *NISLC26A10* contained 11 transmembrane regions. After RNAi, the follicle cells expression of *NISLC26A10* was attenuated by ds*NISLC26A10* and its morphology was shriveled (**Figures 8A,B,E,F**). Similarly, the expression of *NISLC26A10* at the gut cell membranes was weakened after ds*NISLC26A10* treatment (**Figures 8C,D,G,H**).

Effects of RNAi on Genes Related to Ovarian Development

The changes in the transcription level of some genes are related to ovarian development after RNAi. Vitellogenin (Vg) and the vitellogenin receptor (VgR) are important in the reproductive development of insects and act key roles in ovarian development (Cong et al., 2015; Shang et al., 2018; Hu et al., 2019; Zou et al., 2020). The relative expression levels of Vg and VgR

were detected after ds*NISLC26A10* and ds*GFP* treatments. The results showed the Vg expression level in the ds*NISLC26A10* treatment was markedly decreased at 3 and 5 d.p.i. (**Figure 9A**), and the expression level of VgR had a marked decrease at 2 and 3 d.p.i. (**Figure 9B**) compared with the ds*GFP* treatment. These indicate RNAi of *NISLC26A10* reduces the expression of Vg and VgR in *N. lugens*.

Because the synthesis of insect Vg is generally regulated by juvenile hormones (JH; Song et al., 2014; Lyu et al., 2019; Gijbels et al., 2020), and JH plays major roles in development, ovary maturation, and reproduction in insects (Riddiford et al., 2003), genes related to JH synthesis and degradation were examined, including JHAMT (juvenile hormone acid methyltransferase), FAMET (farnesoic acid O-methyltransferase), and JHE (juvenile hormone esterase). After ds*NISLC26A10* treatment, the expression level of *JHAMT* decreased at 2 d.p.i., and significantly decreased at 3 and 5 d.p.i., compared with the ds*GFP* treatment (**Figure 9C**). Similarly, the expression level of *FAMET* was significantly decreased at 2, 3, and 5 d.p.i. (**Figure 9D**) and *JHE* significantly decreased at 3 d.p.i. (**Figure 9E**). These results indicate that the RNAi *NISLC26A10* affects the expression of Vg by regulating JH.

DISCUSSION

Ovarian development, spawning, and hatchability of eggs were affected by ds*NISLC26A10*. This phenomenon may be attributed to the nutritional signals of reproduction. The normal development of oocytes is important for insects. At present, there have been a large number of studies that verified the role of Vg and VgR in the reproduction and development of insects. Vg participates in the development of the embryo,

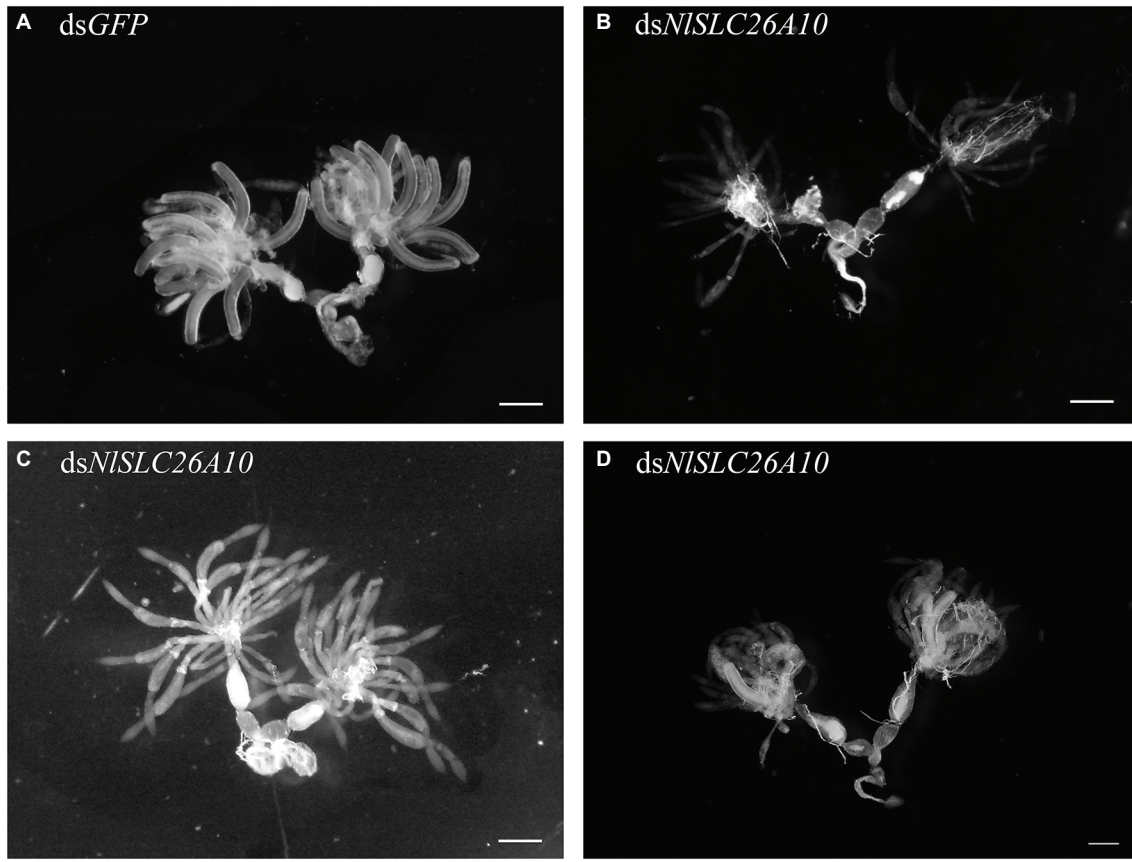


FIGURE 6 | Effects of *dsNISLC26A10* on the ovarian development of *N. lugens*. (A) Ovaries from *dsGFP*-treatment at 5 day post-injection of dsRNA. In (B–D), ovaries were affected to varying extents from *dsNISLC26A10*-treatment at 5 day post-injection of dsRNA. Scale bar: 100 μ m.

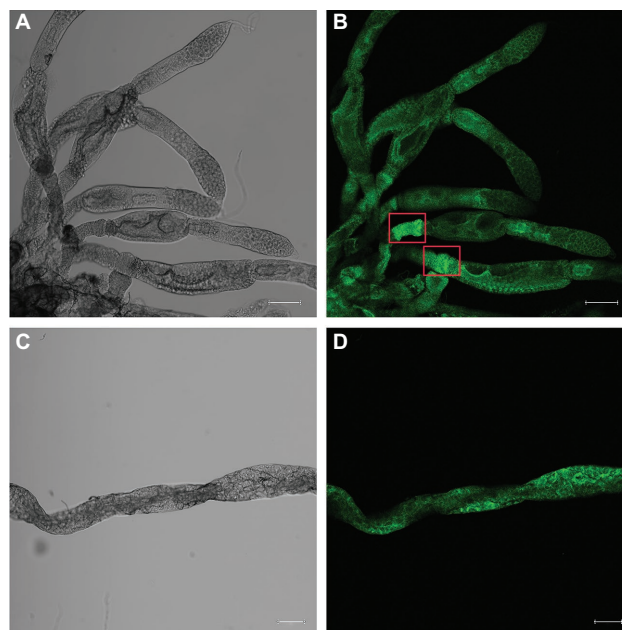


FIGURE 7 | Immunofluorescence analysis of *NISLC26A10* expression in the ovary (A,B) and gut (C,D) of untreated *N. lugens*. Fluorescence signals are stronger in the ovariole pedicels (red boxes in B). The green signal represents the location of *NISLC26A10*. The Scale bar: 100 μ m.

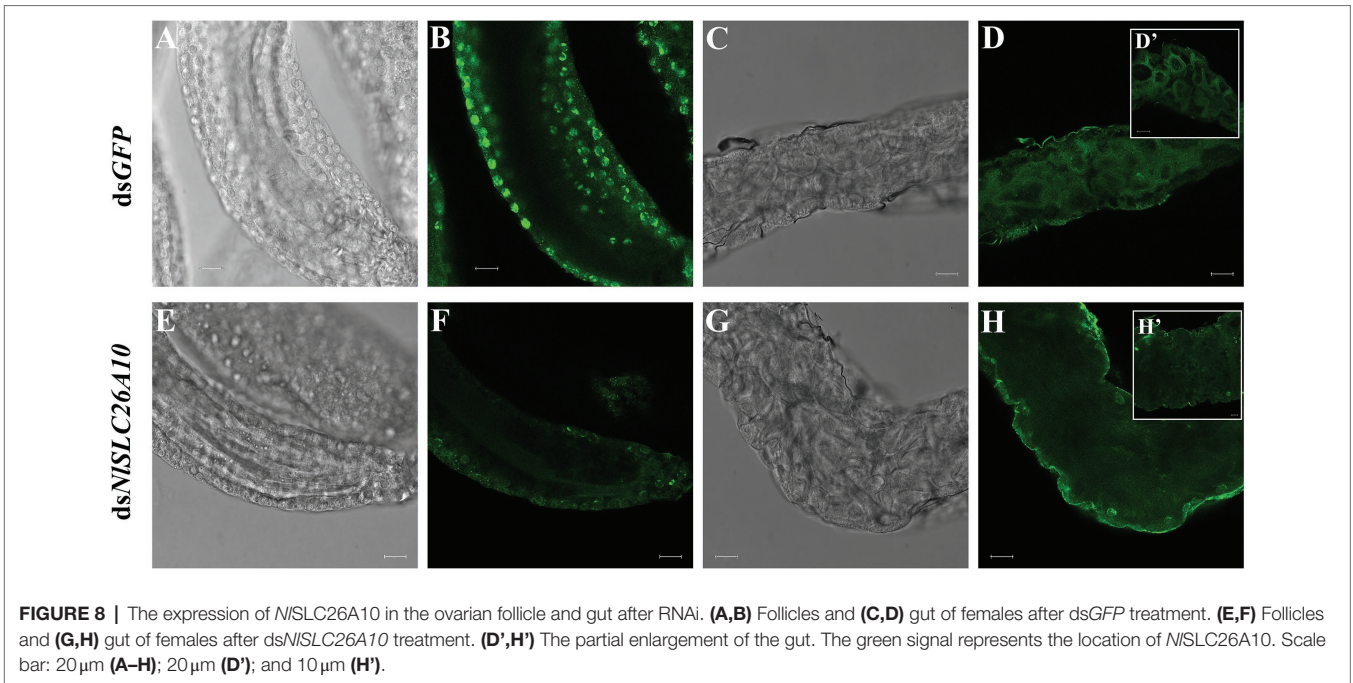


FIGURE 8 | The expression of *NISLC26A10* in the ovarian follicle and gut after RNAi. **(A,B)** Follicles and **(C,D)** gut of females after *dsGFP* treatment. **(E,F)** Follicles and **(G,H)** gut of females after *dsNISLC26A10* treatment. **(D',H')** The partial enlargement of the gut. The green signal represents the location of *NISLC26A10*. Scale bar: 20 μm **(A–H)**; 20 μm **(D')**; and 10 μm **(H')**.

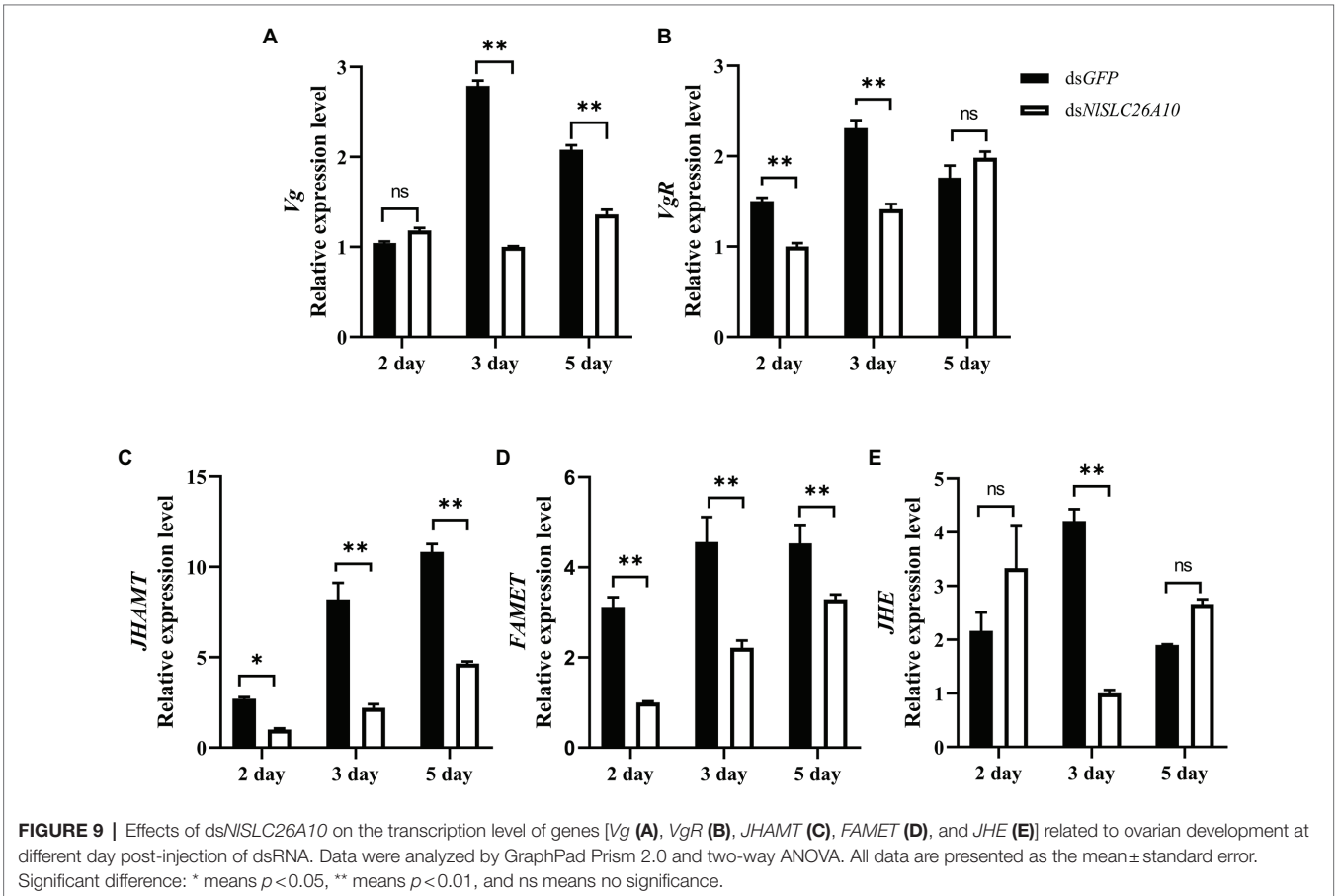


FIGURE 9 | Effects of *dsNISLC26A10* on the transcription level of genes [*Vg* **(A)**, *VgR* **(B)**, *JHAMT* **(C)**, *FAME1* **(D)**, and *JHE* **(E)**] related to ovarian development at different day post-injection of dsRNA. Data were analyzed by GraphPad Prism 2.0 and two-way ANOVA. All data are presented as the mean ± standard error. Significant difference: * means $p < 0.05$, ** means $p < 0.01$, and ns means no significance.

providing nutrition and promoting oocyte development (Sappington and Raikhel, 1998; Tufail and Takeda, 2008). Knockdown of *NIVg* inhibits oocyte growth in the ovarioles, leads to oocyte abnormal development, and females fail to produce offspring (Shen et al., 2019). In the bedbug *Cimex lectularius*, the downregulation of *ClVg* expression causes ovary atrophy and inhibits reproduction (Moriyama et al., 2016). *Vg* is usually synthesized in fat bodies, and *VgR* is responsible for transferring *Vg* into the oocyte (Schneider, 1996). In *Bactrocera dorsalis*, the lack of *VgR* hinders ovary development (Cong et al., 2015). Injection with *dsNIVgR* inhibits spawning and ovary development of *N. lugens* (Lu et al., 2015). In *Agasicles hygrophila*, *dsVgR* injection sharply decreases its fecundity and the ovariole is shortened (Zhang et al., 2019). In *Aphis citricidus*, silencing the *Vg*- and *VgR*-associated genes leads to delayed embryonic development (Shang et al., 2018). TOR (Target of rapamycin) is a signal molecule, which is responsible for the regulation of cell growth in eukaryotes. In the mosquito *Aedes aegypti*, *AaTOR* knockdown reduces the *Vg* gene expression level, thus inhibiting egg development (Hansen et al., 2004). In *N. lugens*, adults injected with *dsTOR* have lower fecundity as affected by *Vg* (Zhai et al., 2015). *NLIInR1* and *NLIInR2* knockdown in *N. lugens* reduce the expression of *Vg* and *VgR* and hamper ovarian development (Liu et al., 2020). Similar results were observed in our experiments. RNAi of *NISLC26A10* resulted in a significant expression decrease for *Vg* and *VgR*. We speculated that downregulated *NISLC26A10* expression resulted in lower expression of *Vg* and thus follicles cannot develop. Lower expression of *VgR* disrupted uptake of *Vg* into the developing oocyte, thereby inhibited ovarian development.

Vg expression in *N. lugens* is correlated with the regulation of JH (Lu et al., 2016; Ge et al., 2017). During the synthesis and degradation of JH in insects, JHAMT is a key rate-limiting enzyme at the final step of the JH biosynthesis pathway (Nie et al., 2014). FAME1 is involved in the final rate-limiting step (Nagaraju, 2007; Zhang et al., 2021), and JHE is used to degrade JH (Zhang et al., 2017). FAME1 and JHE are two key enzymes in the synthesis and metabolism of JH, respectively. RNAi-mediated silence of *N. lugens jmtN* (*JHAMT*) reduces the *Vg* gene expression level, suppresses the maturation of oocytes, and lowers fecundity (Lu et al., 2016). In *Tribolium castaneum*, *dsJHAMT* injection reduces the *Vg* gene expression level (Parthasarathy et al., 2010; Sheng et al., 2011). RNAi of *FAME1* reduces *Vg* expression of *riochair sinensis* and *Macrobrachium rosenbergii* (Qian and Liu, 2019; Chen et al., 2021). In *Apis mellifera*, injection with *dsAmJHE-like* significantly reduces *Vg* transcript levels (Lourenço et al., 2019). Regulation of downstream or upstream genes of JH also affects JH level and *Vg* expression. Methoprene-tolerant (*Met*) is a universal JH receptor. Silencing *GdMet* inhibits the expression of *JHE* and *Vg*, causing reproductive diapause of *Galeruca daurica* (Ma et al., 2021). Adenyl cyclase (*AC*) plays a role in cell signaling processes. Silencing *NIAC9* (the *N. lugens AC like-9* gene) reduces JH concentration, reduces *Vg* expression, and decreases the number of eggs laid of *N. lugens* (Ge et al., 2017). In the present study, we found *JHAMT*, *FAME1*, and *JHE* expression were

significantly decreased by *dsNISLC26A10* treatment. Combining the above results that *Vg* expression and ovarian development were affected by *dsNISLC26A10*, this indicates RNAi of *NISLC26A10* results in the decrease of JH levels and then leads to the decrease of *Vg* expression and hinders the ovarian development of *N. lugens*.

Even though the function of SLC26A10 has not been reported yet, considering SLC26A10 is an anion exchanger and its high expression in the ovary, the relation of *NISLC26A10* to the phenomena found at the present study might be explained as follows. (1) RNAi of *NISLC26A10* induces ion homeostasis, thus weaken the functions of some ion-dependent upstream regulator of JH expression. (2) RNAi of *NISLC26A10* affects the anions secretion and absorption of oocytes in *N. lugens*, obstructing the transport of substances related to ovarian development, then hinders the maturation of the ovary. An example in the Indian white shrimp *Penaeus indicus* is as: a solute carrier, *SLC15A4*, transports amino acids to target regions to help endocrine signaling to stimulate faster ovarian maturation (Saikrithi et al., 2020). (3) After *NISLC26A10* is silenced, its STAS domain is destroyed; then, the interaction protein-protein interaction and ion homeostasis on the oocyte surface would be disrupted, consequently damage the biological function of the oocyte, and hinder ovarian development, because the STAS domain is essential in intracellular transport and protein-protein interactions, and its mutations cause the inefficient transport of sulfate into the cells (Shibagaki and Grossman, 2006).

After *dsNISLC26A10* treatment, the number of YLSs entering the oocytes was also lower. RNAi of *NISLC26A10* may result in the potential change of cytomembrane, thereby reducing YLSs' movement to the ovary. From another perspective, RNAi of *NISLC26A10* downregulates the *Vg* expression, and then affects the entry of YLSs into the ovary, because vitellogenesis indirectly affects YLSs entering the ovary (Nan et al., 2016). Considering YLSs are primary symbionts and provide nutrients for *N. lugens* (Pang et al., 2012; Ge et al., 2016), the decrease in YLSs number in mature oocytes may cause the reduced hatchability of eggs.

CONCLUSION

In this study, we cloned and characterized *NISLC26A10*. The RNAi-mediated knockdown of *NISLC26A10* revealed negative effects on ovarian development, spawning, and hatchability of eggs in *N. lugens*. This indicates that *NISLC26A10* plays an important role in the reproductive development of *N. lugens*. This effect may be through regulating the synthesis of JH, thereby affecting the expression of *Vg*, or through influencing the transovarial transmission of YLSs thereby affecting the hatching of eggs.

DATA AVAILABILITY STATEMENT

The datasets presented in this study can be found in online repositories. The names of the repository/repositories and accession number(s) can be found in the article/**Supplementary Material**.

AUTHOR CONTRIBUTIONS

RZ and YX: conceptualization. RZ, JJ, YL, and JY: investigation. RZ: validation. YX and XY: supervision. RZ: writing—original draft. YX: writing—review and editing. All authors contributed to the article and approved the submitted version.

FUNDING

This work was supported by grants from the National Natural Science Foundation of China (31871961, U21A20223, and

31501632), Zhejiang Provincial Key R&D Project (2019C02015 and 2022C02047), Natural Science Foundation of Zhejiang Province (LY22C140007), and Fundamental Research Funds for the Provincial Universities of Zhejiang (2020YW14).

SUPPLEMENTARY MATERIAL

The Supplementary Material for this article can be found online at: <https://www.frontiersin.org/articles/10.3389/fphys.2022.853956/full#supplementary-material>

REFERENCES

- Alper, S. L., and Sharma, A. K. (2013). The SLC26 gene family of anion transporters and channels. *Mol. Asp. Med.* 34, 494–515. doi: 10.1016/j.mam.2012.07.009
- Alvarez, B. V., Kieller, D. M., Quon, A. L., Markovich, D., and Casey, J. R. (2004). Slc26a6: a cardiac chloride-hydroxyl exchanger and predominant chloride-bicarbonate exchanger of the mouse heart. *J. Physiol.* 561, 721–734. doi: 10.1113/jphysiol.2004.077339
- Andharia, N., Hayashi, M., and Matsuda, H. (2018). Electrophysiological properties of anion exchangers in the luminal membrane of Guinea pig pancreatic duct cells. *Pflugers Arch.* 470, 897–907. doi: 10.1007/s00424-018-2116-1
- Bao, Y. Y., and Zhang, C. X. (2019). Recent advances in molecular biology research of a rice pest, the brown planthopper. *J. Integr. Agric.* 18, 716–728. doi: 10.1016/S2095-3119(17)61888-4
- Bottrell, D. G., and Schoenly, K. G. (2012). Resurrecting the ghost of green revolutions past: the brown planthopper as a recurring threat to high-yielding rice production in tropical Asia. *J. Asia Pac. Entomol.* 15, 122–140. doi: 10.1016/j.aspen.2011.09.004
- Chen, T., Xu, R., Sheng, N., Che, S., Zhu, L., Liu, F., et al. (2021). Molecular evidence for farnesoic acid O-methyltransferase (FAMeT) involved in the biosynthesis of vitellogenin in the Chinese mitten crab *Eriocheir sinensis*. *Anim. Reprod. Sci.* 234:106868. doi: 10.1016/j.anireprosci.2021.106868
- Cheng, D. J., and Hou, R. F. (2001). Histological observations on transovarial transmission of a yeast-like symbiote in *Nilaparvata lugens* Stal (Homoptera, Delphacidae). *Tissue Cell* 33, 273–279. doi: 10.1054/tice.2001.0173
- Cong, L., Yang, W. J., Jiang, X. Z., Niu, J. Z., Shen, G. M., Ran, C., et al. (2015). The essential role of vitellogenin receptor in ovary development and vitellogenin uptake in *Bactrocera dorsalis* (Hendel). *Int. J. Mol. Sci.* 16, 18368–18383. doi: 10.3390/ijms160818368
- Ge, L., Gu, H., Huang, B., Song, Q., Stanley, D., Liu, F., et al. (2017). An adenylyl cyclase like-9 gene (NIAC9) influences growth and fecundity in the brown planthopper, *Nilaparvata lugens* (Stal) (Hemiptera: Delphacidae). *PLoS One* 12:e0189214. doi: 10.1371/journal.pone.0189214
- Ge, L. Q., Xia, T., Huang, B., Song, Q. S., Zhang, H. W., Stanley, D., et al. (2016). Suppressing male spermatogenesis-associated protein 5-like gene expression reduces vitellogenin gene expression and fecundity in *Nilaparvata lugens* Stal. *Sci. Rep.* 6:28111. doi: 10.1038/srep28111
- Gijbels, M., Schellens, S., Schellekens, T., Bruyninckx, E., Marchal, E., and Vanden Broeck, J. (2020). Precocious downregulation of kruppel-homolog 1 in the migratory locust, *Locusta migratoria*, gives rise to an adultoid phenotype with accelerated ovarian development but disturbed mating and oviposition. *Int. J. Mol. Sci.* 21:6058. doi: 10.3390/ijms21176058
- Hansen, I. A., Attardo, G. M., Park, J. H., Peng, Q., and Raikhel, A. S. (2004). Target of rapamycin-mediated amino acid signaling in mosquito anautogeny. *Proc. Natl. Acad. Sci. U. S. A.* 101, 10626–10631. doi: 10.1073/pnas.0403460101
- Heong, K. L., and Hardy, B. (2009). *Planthoppers: New Threats to the Sustainability of Intensive Rice Production Systems in Asia*. Los Baños, Philippines: International Rice Research Institute
- Houk, E. J., and Griffiths, G. W. (1980). Intracellular symbiotes of the Homoptera. *Annu. Rev. Entomol.* 25, 161–187. doi: 10.1146/annurev.en.25.010180.001113
- Hu, K., Tian, P., Tang, Y., Yang, L., Qiu, L., He, H., et al. (2019). Molecular characterization of vitellogenin and its receptor in *Sogatella furcifera*, and their function in oocyte maturation. *Front. Physiol.* 10:1532. doi: 10.3389/fphys.2019.01532
- Knight, M. I., Daetwyler, H. D., Hayes, B. J., Hayden, M. J., Ball, A. J., Pethick, D. W., et al. (2012). Discovery and trait association of single nucleotide polymorphisms from gene regions of influence on meat tenderness and long-chain omega-3 fatty acid content in Australian lamb. *Anim. Prod. Sci.* 52, 591–600. doi: 10.1071/AN11229
- Liu, Y. K., Luo, Y. J., Deng, Y. M., Li, Y., Pang, X. Q., Xu, C. D., et al. (2020). Insulin receptors regulate the fecundity of *Nilaparvata lugens* (Stål) (Hemiptera: Delphacidae). *J. Asia Pac. Entomol.* 23, 1151–1159. doi: 10.1016/j.aspen.2020.09.011
- Lourenço, A. P., Martins, J. R., Torres, F., Mackert, A., Aguiar, L. R., Hartfelder, K., et al. (2019). Immunosenescence in honey bees (*Apis mellifera* L.) is caused by intrinsic senescence and behavioral physiology. *Exp. Gerontol.* 119, 174–183. doi: 10.1016/j.exger.2019.02.005
- Lu, K., Chen, X., Liu, W. T., Zhang, X. Y., Chen, M. X., and Zhou, Q. (2016). Nutritional signaling regulates vitellogenin synthesis and egg development through juvenile hormone in *Nilaparvata lugens* (Stal). *Int. J. Mol. Sci.* 17:269. doi: 10.3390/ijms17030269
- Lu, K., Shu, Y., Zhou, J., Zhang, X., Zhang, X., Chen, M., et al. (2015). Molecular characterization and RNA interference analysis of vitellogenin receptor from *Nilaparvata lugens* (Stal). *J. Insect Physiol.* 73, 20–29. doi: 10.1016/j.jinsphys.2015.01.007
- Lyu, Z., Li, Z., Cheng, J., Wang, C., Chen, J., and Lin, T. (2019). Suppression of gene juvenile hormone diol kinase delays pupation in *Heortia vitessoides* Moore. *Insects* 10:278. doi: 10.3390/insects10090278
- Ma, H. Y., Li, Y. Y., Li, L., Tan, Y., and Pang, B. P. (2021). Juvenile hormone regulates the reproductive diapause through methoprene-tolerant gene in *Galeruca daurica*. *Insect Mol. Biol.* 30, 446–458. doi: 10.1111/imb.12710
- Milligan, J. F., Groebe, D. R., Witherell, G. W., and Uhlenbeck, O. C. (1987). Oligoribonucleotide synthesis using T7 RNA polymerase and synthetic DNA templates. *Nucleic Acids Res.* 15, 8783–8798. doi: 10.1093/nar/15.21.8783
- Moriyama, M., Hosokawa, T., Tanahashi, M., Nikoh, N., and Fukatsu, T. (2016). Suppression of bedbug's reproduction by RNA interference of vitellogenin. *PLoS One* 11:e0153984. doi: 10.1371/journal.pone.0153984
- Mount, D. B., and Romero, M. F. (2004). The SLC26 gene family of multifunctional anion exchangers. *Pflugers Arch.* 447, 710–721. doi: 10.1007/s00424-003-1090-3
- Nagaraju, G. P. C. (2007). Is methyl farnesoate a crustacean hormone? *Aquaculture* 272, 39–54. doi: 10.1016/j.aquaculture.2007.05.014
- Nan, G. H., Xu, Y. P., Yu, Y. W., Zhao, C. X., Zhang, C. X., and Yu, X. P. (2016). Oocyte vitellogenesis triggers the entry of yeast-like symbionts into the oocyte of brown planthopper (Hemiptera: Delphacidae). *Ann. Entomol. Soc. Am.* 109, 753–758. doi: 10.1093/aesa/saw025
- Nie, H., Liu, C., Cheng, T., Li, Q., Wu, Y., Zhou, M., et al. (2014). Transcriptome analysis of integument differentially expressed genes in the pigment mutant (*quail*) during molting of silkworm, *Bombyx mori*. *PLoS One* 9:e94185. doi: 10.1371/journal.pone.0094185
- Noda, H., Nakashima, N., and Koizumi, M. (1995). Phylogenetic position of yeast-like symbiotes of rice planthoppers based on partial 18S rDNA sequences. *Insect Biochem. Mol. Biol.* 25, 639–646. doi: 10.1016/0965-1748(94)00107-S

- Ohana, E., Yang, D., Shcheynikov, N., and Muallem, S. (2009). Diverse transport modes by the solute carrier 26 family of anion transporters. *J. Physiol.* 587, 2179–2185. doi: 10.1113/jphysiol.2008.164863
- Pang, K., Dong, S. Z., Hou, Y., Bian, Y. L., Yang, K., and Yu, X. P. (2012). Cultivation, identification and quantification of one species of yeast-like symbiotes, *Candida*, in the rice brown planthopper, *Nilaparvata lugens*. *Insect Sci.* 19, 477–484. doi: 10.1111/j.1744-7917.2011.01486.x
- Parthasarathy, R., Sun, Z., Bai, H., and Palli, S. R. (2010). Juvenile hormone regulation of vitellogenin synthesis in the red flour beetle, *Tribolium castaneum*. *Insect Biochem. Mol. Biol.* 40, 405–414. doi: 10.1016/j.ibmb.2010.03.006
- Qian, Z., and Liu, X. (2019). Elucidation of the role of farnesoic acid O-methyltransferase (FAME_T) in the giant freshwater prawn, *Macrobrachium rosenbergii*: possible functional correlation with ecdysteroid signaling. *Comp. Biochem. Physiol. A Mol. Integr. Physiol.* 232, 1–12. doi: 10.1016/j.cbpa.2019.03.003
- Riddiford, L. M., Hiruma, K., Zhou, X., and Nelson, C. A. (2003). Insights into the molecular basis of the hormonal control of molting and metamorphosis from *Manduca sexta* and *Drosophila melanogaster*. *Insect Biochem. Mol. Biol.* 33, 1327–1338. doi: 10.1016/j.ibmb.2003.06.001
- Saikrithi, P., Balasubramanian, C. P., Otta, S. K., and Tomy, S. (2020). Expression dynamics of solute carrier family 15 member 4 (SLC15A4) and its potential regulatory role in ovarian development of the Indian white shrimp, *Penaeus indicus*. *Mol. Biol. Rep.* 47, 3797–3805. doi: 10.1007/s11033-020-05471-x
- Sappington, T. W., and Raikhel, A. S. (1998). Molecular characteristics of insect vitellogenins and vitellogenin receptors. *Insect Biochem. Mol. Biol.* 28, 277–300. doi: 10.1016/S0965-1748(97)00110-0
- Schneider, W. J. (1996). Vitellogenin receptors: oocyte-specific members of the low-density lipoprotein receptor supergene family. *Int. Rev. Cytol.* 166, 103–137. doi: 10.1016/s0074-7696(08)62507-3
- Shang, F., Niu, J. Z., Ding, B. Y., Zhang, Q., Ye, C., Zhang, W., et al. (2018). Vitellogenin and its receptor play essential roles in the development and reproduction of the brown citrus aphid, *Aphis (Toxoptera) citricidus*. *Insect Mol. Biol.* 27, 221–233. doi: 10.1111/imb.12366
- Shen, Y., Chen, Y. Z., Lou, Y. H., and Zhang, C. X. (2019). Vitellogenin and vitellogenin-like genes in the brown planthopper. *Front. Physiol.* 10:1181. doi: 10.3389/fphys.2019.01181
- Sheng, Z., Xu, J., Bai, H., Zhu, F., and Palli, S. R. (2011). Juvenile hormone regulates vitellogenin gene expression through insulin-like peptide signaling pathway in the red flour beetle, *Tribolium castaneum*. *J. Biol. Chem.* 286, 41924–41936. doi: 10.1074/jbc.M111.269845
- Shibagaki, N., and Grossman, A. R. (2006). The role of the STAS domain in the function and biogenesis of a sulfate transporter as probed by random mutagenesis. *J. Biol. Chem.* 281, 22964–22973. doi: 10.1074/jbc.M603462200
- Sindić, A., Chang, M. H., Mount, D. B., and Romero, M. F. (2007). Renal physiology of SLC26 anion exchangers. *Curr. Opin. Nephrol. Hypertens.* 16, 484–490. doi: 10.1097/MNH.0b013e3282e7d7d0
- Sōgawa, K. (1982). The rice brown planthopper: feeding physiology and host plant interactions. *Annu. Rev. Entomol.* 27, 49–73. doi: 10.1146/annurev.en.27.010182.000405
- Song, J., Wu, Z., Wang, Z., Deng, S., and Zhou, S. (2014). Krüppel-homolog 1 mediates juvenile hormone action to promote vitellogenesis and oocyte maturation in the migratory locust. *Insect Biochem. Mol. Biol.* 52, 94–101. doi: 10.1016/j.ibmb.2014.07.001
- Tufail, M., and Takeda, M. (2008). Molecular characteristics of insect vitellogenins. *J. Insect Physiol.* 54, 1447–1458. doi: 10.1016/j.jinsphys.2008.08.007
- Wang, C., Sun, B., Zhang, X., Huang, X., Zhang, M., Guo, H., et al. (2019). Structural mechanism of the active bicarbonate transporter from cyanobacteria. *Nat. Plants* 5, 1184–1193. doi: 10.1038/s41477-019-0538-1
- Whitfield, A. E., and Rotenberg, D. (2015). Disruption of insect transmission of plant viruses. *Curr. Opin. Insect Sci.* 8, 79–87. doi: 10.1016/j.cois.2015.01.009
- Wu, J. M., Zheng, R. E., Zhang, R. J., Ji, J. L., Yu, X. P., and Xu, Y. P. (2019). A clip domain serine protease involved in egg production in *Nilaparvata lugens*: expression patterns and RNA interference. *Insects* 10:378. doi: 10.3390/insects10110378
- Zhai, Y., Sun, Z., Zhang, J., Kang, K., Chen, J., and Zhang, W. (2015). Activation of the TOR signalling pathway by glutamine regulates insect fecundity. *Sci. Rep.* 5:10694. doi: 10.1038/srep10694
- Zhang, H., Liu, Y., Jin, J., Zhou, Z., and Guo, J. (2019). Identification and characterization of the vitellogenin receptor gene and its role in reproduction in the Alligatorweed Flea Beetle, *Agasicles hygrophila*. *Front. Physiol.* 10:969. doi: 10.3389/fphys.2019.00969
- Zhang, L., Li, X., Li, T., Xiong, R., Li, Y., Yan, D., et al. (2021). Farnesoic acid methyltransferase 6 (BmFAME_T6) interrelates with molting of dominant trimolter in silkworm, *Bombyx mori*. *Biologia* 76, 2231–2240. doi: 10.1007/s11756-021-00707-y
- Zhang, Z., Liu, X., Shiotsuki, T., Wang, Z., Xu, X., Huang, Y., et al. (2017). Depletion of juvenile hormone esterase extends larval growth in *Bombyx mori*. *Insect Biochem. Mol. Biol.* 81, 72–79. doi: 10.1016/j.ibmb.2017.01.001
- Zheng, L., Mao, Q., Xie, L., and Wei, T. (2014). Infection route of rice grassy stunt virus, a tenuivirus, in the body of its brown planthopper vector, *Nilaparvata lugens* (Hemiptera: Delphacidae) after ingestion of virus. *Virus Res.* 188, 170–173. doi: 10.1016/j.virusres.2014.04.008
- Zou, M. M., Wang, Q., Chu, L. N., Vasseur, L., Zhai, Y. L., Qin, Y. D., et al. (2020). CRISPR/Cas9-induced vitellogenin knockout lead to incomplete embryonic development in *Plutella xylostella*. *Insect Biochem. Mol. Biol.* 123:103406. doi: 10.1016/j.ibmb.2020.103406

Conflict of Interest: The authors declare that the research was conducted in the absence of any commercial or financial relationships that could be construed as a potential conflict of interest.

Publisher's Note: All claims expressed in this article are solely those of the authors and do not necessarily represent those of their affiliated organizations, or those of the publisher, the editors and the reviewers. Any product that may be evaluated in this article, or claim that may be made by its manufacturer, is not guaranteed or endorsed by the publisher.

Copyright © 2022 Zhang, Ji, Li, Yu, Yu and Xu. This is an open-access article distributed under the terms of the Creative Commons Attribution License (CC BY). The use, distribution or reproduction in other forums is permitted, provided the original author(s) and the copyright owner(s) are credited and that the original publication in this journal is cited, in accordance with accepted academic practice. No use, distribution or reproduction is permitted which does not comply with these terms.